44. Simulation and stability of multi-port DC-DC converter

Samir Al Sharif[1], Zhijun Qian[2], Ahmad Harb[3], Issa Batarseh[4]
[1]Electrical Engineering Department at Taibah University, Madinah, KSA
[2, 4]Electrical Engineering and Computer Science Dept. at University of Central Florida, Orlando, FL, USA
[3]Energy Engineering Department at German Jordanian University, Amman, Jordan
[3]Corresponding author
E-mail: [3]*aharb48@gmail.com*

(Received 3 December 2013; received in revised form 15 April 2014; accepted 27 April 2014)

Abstract. In this paper, the simulation and stability of multi-port DC-DC converter will be presented. Traditional DC-DC converter topologies interface two power terminals: a source and a load. The construction of diverse and flexible power management and distribution systems with such topologies is governed by a tight compromise between converter count, efficiency, and control complexity. The DC-DC converter may be considered as an advanced environment-friendly electronic conversion system, since it is a greenhouse emission eliminator. By utilizing the advancement of these renewable energy sources, we minimize the use of fossil fuel and thus contribute to a cleaner and pollution-free environment. Finally, comparison between the averaged model and the actual switching converter model is been studied.

Keywords: multi-port DC-DC converter, simulation.

1. Introduction

Integrated power electronic converters are important for systems that are capable of harvesting power from solar sources, fuel cells, and mechanical vibrations used in applications such as communication repeater stations, sensor networks, hybrid electric vehicles and laptops. Furthermore, multi-terminal interface is important since such systems require mass energy storage to compensate for the mismatch between the sourcing and loading power patterns over a regular operational cycle. For example, a solar system, consisting of a regulated load interfaced to a solar array, requires storage batteries for storing excess power and re-supplying it to the load when needed. Limited research activities on multi-terminal converter topologies have been reported in open literature, with very few commercially installed systems in industry. Interesting ideas for multi-sourced converters with multiple control variables have been introduced based on the flyback (buck-boost) converter topology. As shown in Fig. 1, a three-port dc-dc converter has been proposed in [20] to have bidirectional and also ZVS capabilities. It is based on full bridge cells that allow bidirectional power flow in each port. Such a configuration facilitates the matching of different voltage levels in the overall system by the multi-winding transformer. The transformer design was optimally performed in order to incorporate the leakage inductances as required by the topology to affect the phase shift control. Furthermore, for the three-port converter, a dual-PI-loop based control strategy is proposed to achieve constant output voltage and power flow management. This topology has been verified through a hybrid fuel cell and super-capacitor system to improve the slow transient response of a fuel cell stack.

As shown in Fig. 2, a half-bridge version of this multi-port converter has been proposed in [12] for a fuel cell and super-capacitor generation system. The topology comprises a high-frequency three-winding transformer and three half-bridge cells, one of which is a boost half-bridge. The converter is controlled by phase shift, which achieves the primary power flow control, in combination with pulse width modulation (PWM). With the PWM control it is possible to reduce the rms loss and to extend the zero-voltage switching operating range to the entire phase shift region. A control scheme based on multiple PI regulators manages the power flow, regulates the output, and adjusts the duty cycle in response to the varying voltage on the port. Compared with full-bridge based topology, it applies half input voltage to the transformer and adopts fewer

switches to process the power. For this reason, the half-bridge based multi-port topology is more suitable for low to medium power applications.

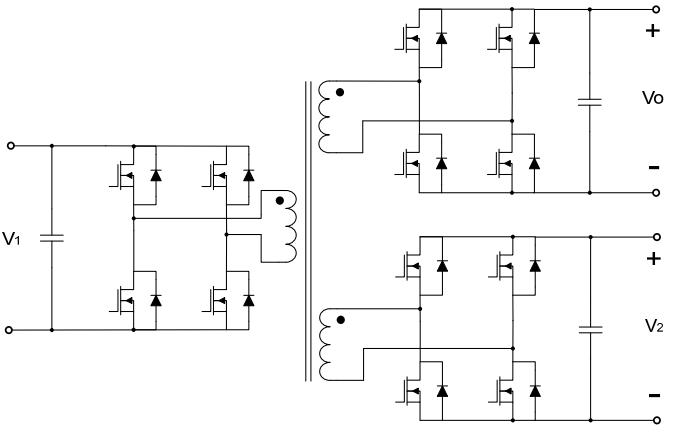

Fig. 1. Three-port full-bridge DC-DC converter

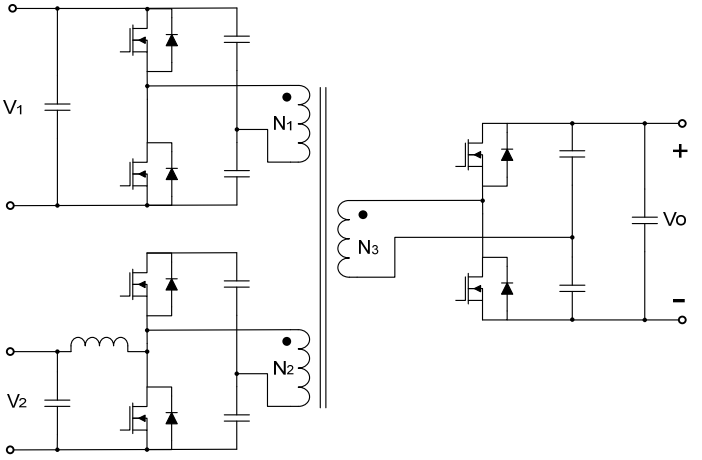

Fig. 2. Three-port half-bridge DC-DC converter

As shown in Fig. 3, a similar topology has been used in [18] to interface hybrid energy storage as the battery and ultra-capacitor to achieve high overall performance. It can interface current source input, and can achieve ZVS for all six main switches by the phase shift control. This paper also discusses the power topology operation and the control aspects of dynamic characteristics analysis and the control strategy.

The above-mentioned topologies adopt a multi-winding transformer to couple different power ports. Therefore, all ports are fully isolated with each other. However, some applications do not require all ports to be fully isolated, and the share of some grounds may allow less component and fewer transformer windings. As shown in Fig. 4, a topology in [10] is intended for future hybrid and fuel cell vehicles which may have three voltage nets: 14 V, 42 V and high voltage (> 200 V) buses. A soft-switched DC-DC converter using four switches has been proposed to interconnect these three nets. Its power flow management is based on a combined duty ratio and phase shift control, but soft-switching range is limited when the phase shifts between two very different voltage levels to have large current swing.

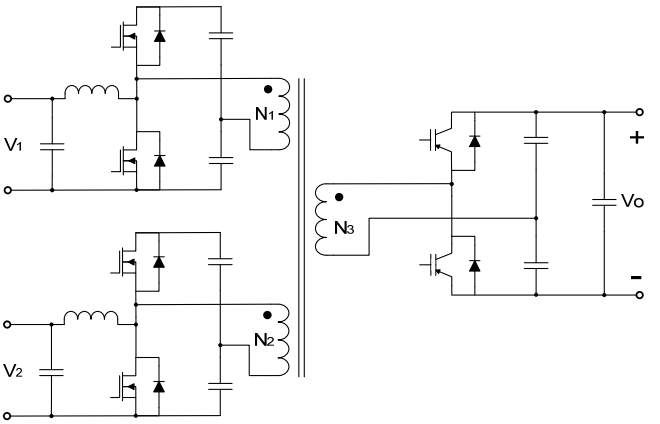

Fig. 3. Triple-half-bridge bidirectional DC-DC converter

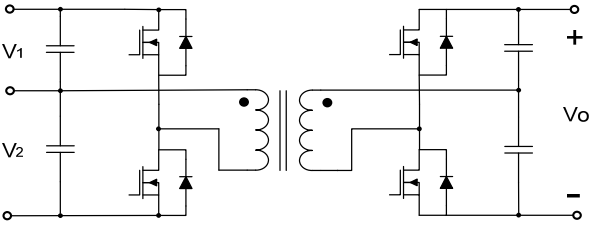

Fig. 4. Reduced part, triple-half-bridge bidirectional DC-DC converter

To sum up, these multi-port topologies can be classified into two categories: non-isolated topologies [1-10] and isolated topologies [10-23]. Non-isolated multi-port converters usually take the form of buck, boost, buck-boost, etc, featuring compact design and high power density; isolated multi-port converters using bridge topologies have the advantages of flexible voltage levels and high efficiency since high frequency transformer and soft-switching techniques are used. Also, isolation may be required for certain critical applications.

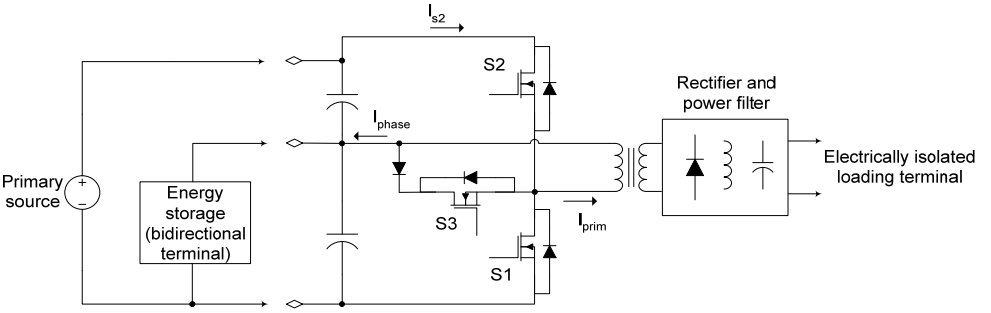

Fig. 5. Three-port proposed DC-DC converter topology

2. Analysis, modeling and control of multi-port DC-DC converter proposed topology

In this paper, the three-port DC-DC Converter, shown in Fig. 5, is proposed. It is a modified version of the PWM half bridge converter that includes three basic circuit stages within a constant-frequency switching cycle to provide two independent control variables. The switching

sequence shown in the figure ensures a clamping path for the energy of the leakage inductance of the transformer at all times. This energy is further utilized to achieve zero-voltage switching (ZVS) for all primary switches for a wide range of source and load conditions.

2.1. Analysis of DC-DC multi-port converter

Full-bridge converters are more suitable for higher power applications, typically above 1 kW. Applying the same concept of dual use of the phase legs, a three-terminal topology can be derived from the full-bridge circuit. The bidirectional terminal of this topology is controlled by changing the duty cycle of the phase legs to achieve the target voltage ratio. The two phase legs need to maintain equal duty cycles. The load terminal is controlled by phase shifting the driving waveforms of these two phase legs relative to each other, just like the mother ZVT full-bridge topology.

The steady-state voltage relationships, assuming CCM operation of the load filter inductor, are given by:

$$V_{bi} = DV_{in},$$
$$V_0 = 2n\phi V_{in},$$

given that $0 \leq \phi \leq \min(D, 1-D)$, where: D is the duty cycle of each phase leg, ϕ is the phase shift between the two phase leg waveforms.

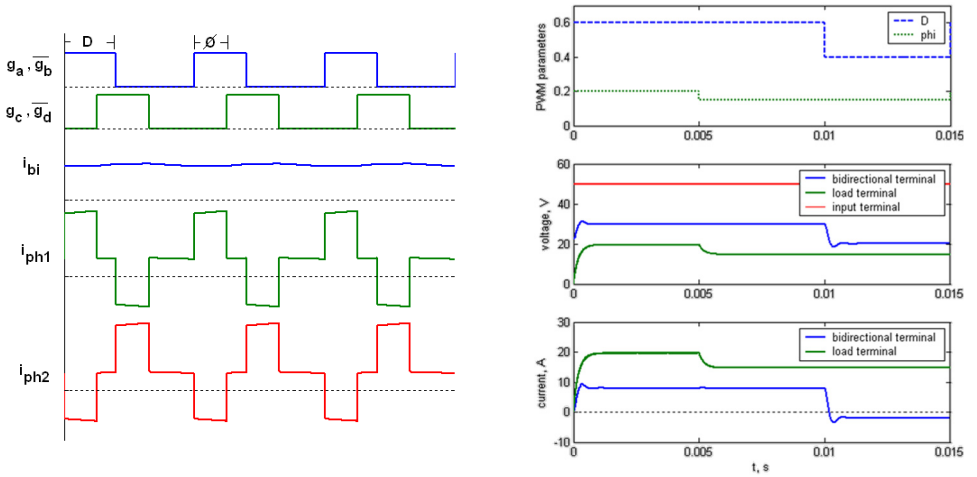

a) b)

Fig. 6. Simulation waveforms a) basic switching waveforms b) terminal voltages and currents

This topology operates as boost-derived push-pull converter when supplying energy from the bidirectional terminal to the load. This topology is thus an attractive alternative for low voltage storage devices since it saves on the turns-ratio of the transformer and simplifies its design. The center-tapped transformer and the bidirectional terminal inductor assembly is suitable for being wound on a single core, in an integrated magnetic fashion.

Simulation results are shown in Fig. 6. Again, control was adjusted at $t = 5$ ms and at 10 ms to independently control the voltages of the load and bidirectional terminals. Converter ability to handle negative current in the bidirectional terminal was verified.

3. Small signal average model

The small signal model is tailored for deriving multi-port DC-DC converters under different

modes of operation. It would be difficult to define different modes since there are various modes of operation. After we define the model therefore, a competitive method is used to realize smooth and seamless mode transition.

3.1. Analysis of multi-port DC-DC converter modeling

In this section we derive small signal transfer functions of the proposed DC-DC converter based on the state equations for four energy storage elements during each circuit stage. The storage elements are battery capacitor C_1, the transformer magnetizing inductance L_m, the output inductance L_o, and the output capacitance C_o. In Fig. 7 the three main circuit stages are shown.

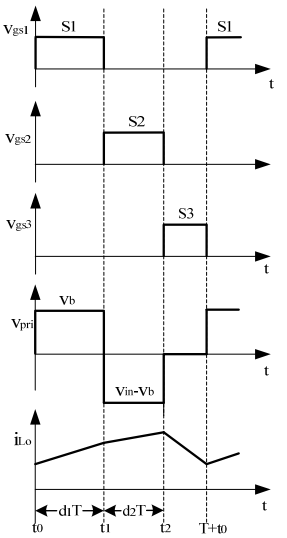

Fig. 7. Basic waveforms of the multi-port converter

In stage I ($t_0 - t_1$), S1 is gated ON and the state equation is derived as follows:

$$\begin{cases} C_1 \cdot \dfrac{dv_{C1}}{dt} = \dfrac{-v_{C1}}{R_b} + i_{Lm} + n \cdot i_{Lo}, \\ L_m \cdot \dfrac{di_{Lm}}{dt} = -v_{C1}, \\ L_o \cdot \dfrac{di_{Lo}}{dt} = v_{C1} \cdot n - v_o, \\ C_o \cdot \dfrac{dv_o}{dt} = i_{Lo} - \dfrac{v_o}{R}. \end{cases}$$

While stage II ($t_1 - t_2$), S2 is gated ON, the state equation is found to be as follows:

$$\begin{cases} C_1 \cdot \dfrac{dv_{C1}}{dt} = \dfrac{-v_{C1}}{R_b} + i_{Lm} + n \cdot i_{Lo}, \\ L_m \cdot \dfrac{di_{Lm}}{dt} = v_{C2} - v_{C1}, \\ L_o \cdot \dfrac{di_{Lo}}{dt} = (v_{C2} - v_{C1}) \cdot n - v_o, \\ C_o \cdot \dfrac{dv_o}{dt} = i_{Lo} - \dfrac{v_o}{R}. \end{cases}$$

In stage III ($t_2 - T + t_0$), S3 is gated ON, the state equation is derived as follows:

$$\begin{cases} C_1 \cdot \dfrac{dv_{C1}}{dt} = \dfrac{-v_{C1}}{R_b}, \\ L_m \cdot \dfrac{di_{Lm}}{dt} = 0, \\ L_o \cdot \dfrac{di_{Lo}}{dt} = -v_o, \\ C_o \cdot \dfrac{dv_o}{dt} = i_{Lo} - \dfrac{v_o}{R}. \end{cases}$$

Let us add small perturbation $\hat{x}$ to state X, one can found:

$$x = X + \hat{x}, \;\; d = D + \hat{d}, \;\; v = V + \hat{v},$$

where $\hat{d} \ll D, \hat{v} \ll V$.

Now, apply the averaging method to the three state equations and neglect second order terms, one obtains:

$$\begin{cases} C_1 \cdot \dfrac{d\hat{v}_{C1}}{dt} = \dfrac{-\hat{v}_{C1}}{R_b} + \hat{\imath}_{Lm}(D_1 + D_2) + n \cdot \hat{\imath}_{Lo}(D_2 - D_1) + I_{Lm}\left(\hat{d}_1 + \hat{d}_2\right) + \dfrac{n \cdot V_0 \cdot \left(\hat{d}_2 + \hat{d}_1\right)}{R}, \\ L_m \cdot \dfrac{d\hat{\imath}_{Lm}}{dt} = -\hat{v}_{C1}(D_1 + D_2) - \dfrac{\left(\hat{d}_1 + \hat{d}_2\right) \cdot D_2 \cdot V_{in}}{(D_1 + D_2)} + \hat{d}_2 \cdot V_{in}, \\ L_o \cdot \dfrac{d\hat{\imath}_{Lo}}{dt} = \hat{v}_{C1} \cdot n \cdot (D_1 + D_2) - \hat{v}_0 + \dfrac{\left(\hat{d}_1 - \hat{d}_2\right) \cdot n \cdot D_2 \cdot V_{in}}{(D_1 + D_2)} + \hat{d}_2 \cdot n \cdot V_{in}, \\ C_o \cdot \dfrac{d\hat{v}_o}{dt} = \hat{\imath}_{Lo} - \dfrac{\hat{v}_o}{R}. \end{cases}$$

Afterwards, the system can be represented in state-space matrix form:

$$\frac{dX}{dt} = A \cdot X + B \cdot U, \;\; Y = I \cdot X,$$

where: X represents the state variables V_{C1}, i_{Lm}, i_{Lo} and V_o, U represents the control inputs d_1 and d_2, Y represents the system outputs, and I stands for the identity matrix:

$$A = \begin{bmatrix} -\dfrac{1}{R_b \cdot C_1} & \dfrac{(D_1 + D_2)}{C_1} & \dfrac{n \cdot (D_1 + D_2)}{C_1} & 0 \\ -\dfrac{(D_1 + D_2)}{L_m} & 0 & 0 & 0 \\ \dfrac{n \cdot (D_1 - D_2)}{L_o} & 0 & 0 & -\dfrac{1}{L_o} \\ 0 & 0 & -\dfrac{1}{C_o} & -\dfrac{1}{R \cdot C_o} \end{bmatrix}, \;\; X = \begin{bmatrix} \hat{v}_{C1} \\ \hat{\imath}_{Lm} \\ \hat{\imath}_{Lo} \\ \hat{v}_o \end{bmatrix},$$

$$B = \begin{bmatrix} \frac{I_{Lm} - n \cdot V_o/R}{C_1} & \frac{I_{Lm} + n \cdot V_o/R}{C_1} \\ -\frac{D_2 \cdot V_{in}}{(D_1 + D_2) \cdot L_m} & \frac{D_1 \cdot V_{in}}{(D_1 + D_2) \cdot L_m} \\ \frac{n \cdot D_2 \cdot V_{in}}{(D_1 + D_2) \cdot L_o} & \frac{n \cdot D_1 \cdot V_{in}}{(D_1 + D_2) \cdot L_o} \\ 0 & 0 \end{bmatrix}, \quad U = \begin{bmatrix} d_1 \\ d_2 \end{bmatrix}.$$

We use MATLAB's Simulink to compare the averaged model with the actual switching converter model as shown in Fig. 8.

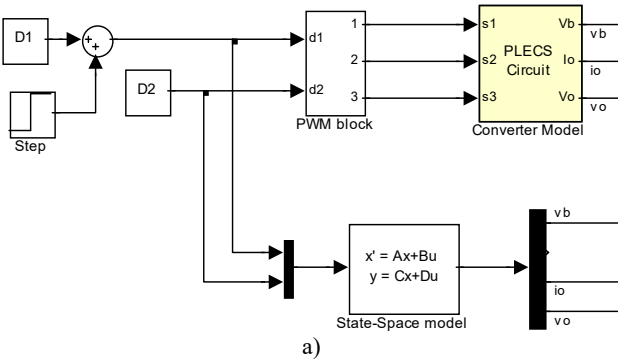

a)

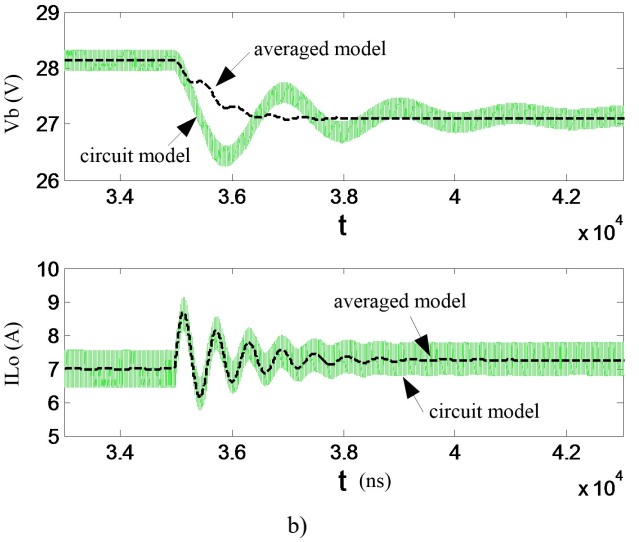

b)

Fig. 8. a) Model comparison due to duty cycle step,
b) Averaged model and circuit model comparison for battery-regulation mode

4. Conclusion

The simulation and stability of a multi-port DC-DC convertor is being presented. The DC-DC converter is considered as an advanced The DC-DC converter may be considered as an advanced environment-friendly electronic conversion system, since it is a greenhouse emission eliminator. By utilizing the advancement of these renewable energy sources, we minimize the use of fossil fuel. At the end a cleaner, pollution free environment is achieved. So, a comparison between the averaged model and the actual switching converter model has been made. The study shows that

the simulations, for both actual and averaged models, are nearly identical.

References

[1] **Di Napoli A., Crescimbini F., Solero L., Caricchi F., Capponi F. G.** Multiple-input DC-DC power converter for power-flow management in hybrid vehicles. IEEE Industry Application Conference, 2002, p. 1578-1585.

[2] **Jiang W., Fahimi B.** Multi-port power electric interface for renewable energy sources. IEEE Applied Power Electronics Conference, 2009, p. 347-352.

[3] **Imes W. G., Rodriguez F. D.** A two-input tri-state converter for spacecraft power conditioning. Proc. AIAA International Energy Conversion Engineering Conference, 1994, p. 163-168.

[4] **Rodriguez F. D., Imes W. G.** Analysis and modeling of a two-input DC/DC converter with two controlled variables and four switched networks. Proc. AIAA International Energy Conversion Engineering Conference, 1994, p. 322-327.

[5] **Dobbs B. G., Chapman P. L.** A multiple-input DC-DC converter topology. IEEE Power Electronics Letters, Vol. 1, 2003, p. 6-9.

[6] **Benavides N. D., Chapman P. L.** Power budgeting of a multiple-inputbuck-boost converter. IEEE Trans. Power Electronics, Vol. 20, 2005, p. 1303-1309.

[7] **Matsuo H., Lin W., Kurokawa F., Shigemizuand T., Watanabe N.** Characteristics of the multiple-input DC-DC converter. IEEE Trans. Industrial Applications, Vol. 51, 2004, p. 625-631.

[8] **Solero L., Caricchi F., Crescimbini F., Honorati O., Mezzetti F.** Performance of A 10 kW power electronic interface for combined Wind/PV isolated generating systems. Proc. IEEE Power Electronics Specialists Conference, 1996, p. 1027-1032.

[9] **Solero L., Lidozzi A., Pomilio J. A.** Design of multiple-input power converter for hybrid vehicles. Proc. IEEE Applied Power Electronics Conference, 2004, p. 1145-1151.

[10] **Gui-jia Su, Peng F. Z.** A low cost, triple-voltage bus DC-DC converter for automotive applications. Proc. IEEE Applied Power Electronics Conference, 2005, p. 1015-1021.

[11] **Peng F. Z., Li H., Su G. J., Lawler J. S.** A new ZVS bidirectionaldc-dc converter for fuel cell and battery applications. IEEE Trans. Power Electronics, Vol. 19, 2004, p. 54-65.

[12] **Tao H., Kotsopoulos A., Duarte J. L., Hendrix M. A. M.** Multi-input bidirectional DC-DC converter combining DC-link and magnetic-coupling for fuel cell systems. Proc. IEEE Industry Applications Conference, 2005, p. 2021-2028.

[13] **Chen Y. M., Liu Y. C., Wu F. Y.** Multi-input DC/DC converter based on the multiwinding transformer for renewable energy applications. IEEE Trans. Industrial Applications, Vol. 38, 2002, p. 1096-1104.

[14] **Michon M., Duarte J. L., Hendrix M., Simoes M. G.** A three-port Bi-directional converter for hybrid fuel cell systems. Proc. IEEE Power Electronics Specialists Conference, 2004, p. 4736-4742.

[15] **Matsuo H., Lin W., Kurokawa F., Shigemizu T., Watanabe N.** Characteristic of the multiple-input DC-DC converter. IEEE Trans. Industrial Electronics, Vol. 51, 2004, p. 625-631.

[16] **Al-Atrash H., Tian F., Batarseh I.** Tri-modal half-bridge converter topology for three-port interface. IEEE Trans. Power Electronics, Vol. 22, 2007, p. 341-345.

[17] **Qian Z., Abdel-Rahman O., Reese J., Al-Atrash H., Batarseh I.** Dynamic analysis of three-port DC/DC converter for space applications. Proc. IEEE Applied Power Electronics Conference, 2009, p. 28-34.

[18] **Liu D., Li H.** A ZVS Bi-directional DC-DC converter for multiple energy storage elements. IEEE Trans. Power Electronics, Vol. 21, 2006, p. 1513-1517.

[19] **Zhao C., Round S. D., Kolar J. W.** An isolated three-port bidirectional DC-DC converter with decoupled power flow management. IEEE Trans. Power Electronics, Vol. 21, 2008, p. 2443-2453.

[20] **Tao H., Kotsopoulos A., Duarte J. L., Hendrix M. A. M.** Transformer-coupled multiport ZVS bidirectional DC–DC converter with wide input range. IEEE Trans. Power Electronics, Vol. 23, 2008, p. 771-781.

[21] **Duarte J. L., Hendrix M., Simoes M. G.** Three-port bidirectional converterfor hybrid fuel cell systems. IEEE Trans. Power Electronics, Vol. 22, 2007, p. 480-487.

[22] **Al-Atrash H., Batarseh I.** Boost-integrated phase-shift full-bridge converters for three-port interface. Proc. IEEE Power Electronics Specialists Conference, 2007, p. 2313-2321.

[23] **Al-Atrash H., Pepper M., Batarseh I.** A zero-voltage switching three-port isolated full-bridge converter. Proc. IEEE International Telecommunications Energy Conference, 2006, p. 411-418.